Interpretation of Tunnel Instrumentation for Safety Management Plan Deflagration

Ana Luisa Cezar Rissoli
University of Brasilia, Brasilia, Brazil, ana_rissoli@hotmail.com

André Pacheco de Assis
University of Brasilia, Brasilia, Brazil, aassis@unb.br

SUMMARY: Displacement instrumentation in tunnel construction is the most common mean to monitor tunnel performance and safety. Therefore, the use of the data available in traditional instrumentation can provide information for Safety Management Plan deflagration. Thirty-eight scenarios were simulated in the FEM software PLAXIS 3D Tunnel. These scenarios include deep and shallow tunnels in rock with different geologies, in which the tunnel approaches better or worse materials zones with different lengths inside the mass. Deflection lines, trend lines, displacement vector orientations, face extrusions, displacement indicators and critical strains were adopted to propose patterns to predict the collapse of tunnel openings, thereafter the trigger of the alarm level. Displacement vector orientations were able predict the transition of materials, but triggering alarms from its increase may cause too many false alarms. The increase of extrusion rate suggested a sign of destabilization. For shallow tunnels, the longitudinal distortion index indicator successfully predicted the collapse.

KEYWORDS: Displacements Evaluation, Safety Management Plan, Tunnel Instrumentation, Stability Evaluation.

1 INTRODUCTION

The occupation of underground space has expanded considerably in recent decades, in particular due to the need to provide adequate infrastructure for the development of cities, preserving the surface for nobler uses. Despite this trend, society still shows great aversion to the underground space, linking it to accidents, disasters and human and economic losses. The risks inherent to civil engineering, and especially underground works, require Safety Management Plans during construction and operation of the structure. The reference levels of the instrumentation of expected behavior, alert and emergency to the deflagration of the Safety Management Plan should be sufficiently precise not to generate loss of confidence in the system and, consequently, in the safety of the structure.

Active instrumentation is the main tool of selection of the criteria, being necessary to define standards for evaluation of the activation of attention and crisis alarms. Traditional tunnel

instrumentation evaluations, as time histories and maximum deformations and distortions, and innovative ways, as displacement vector orientation, trend lines and deflection lines, were adopted to propose patterns to predict the collapse of tunnel openings, thereafter the trigger of the alarm level.

Thirty eight scenarios were simulated in the FEM software PLAXIS 3D Tunnel. These scenarios include deep and shallow tunnels in rock with different geologies, in which the tunnel approaches better or worse materials zones with different lengths.

2 MONITORING EVALUATION

The main objectives of instrumentation and monitoring are to obtain information on the response of the ground to the excavation, construction control, verification of the parameters and design models, evaluation of the lining performance during the construction and life cycle of the structure and monitoring of the impact of the work on adjacent structures (ITA, 2011). In addition to these objectives, the instrumentation should also provide information on critical behaviors, predict parameters ahead of the excavation or not yet instrumented and to anticipate the performance of the tunnel as a whole (ITA, 2011), making possible the optimization of the excavation (Moritz et al., 2011).

2.1 Displacements evaluation

Displacements monitoring is the most widespread form of tunneling instrumentation, especially due to the advancement of total stations and data transmission technology, which enabled the monitoring of absolute 3D displacements in a large number of points in a short period of time. The following sections will present how these data are evaluated in tunnel construction.

2.1.1 Time-displacement and distance-displacement diagrams

Time-displacement diagrams are the most traditional plot of displacements, in which vertical, horizontal e longitudinal components are plotted in time. Its main objective is the evaluation of decrease or increase of displacements rates, which characterize the process of stabilization or destabilization (Schubert & Steindorfer, 2004).

Similar to time-displacement diagrams, distance-displacement diagrams show deferent displacements components with distance to face position, also being adopted to evaluate mass stabilization (OGG, 2014). These diagrams are more appropriate way to plot displacements than time-displacements diagrams, because excavation velocities can modify drastically displacements rates, as can be seen in Figure 1. Thus, the change in the rate of advance can generate false interpretation that the section is destabilizing by the increase of displacements rates, which is corrected in the distance-displacement diagram, as can be seen in Figure 1.

Unfortunately, in both diagrams each displacement component of each instrumentation section is plotted individually, not providing a global overview of the excavation.

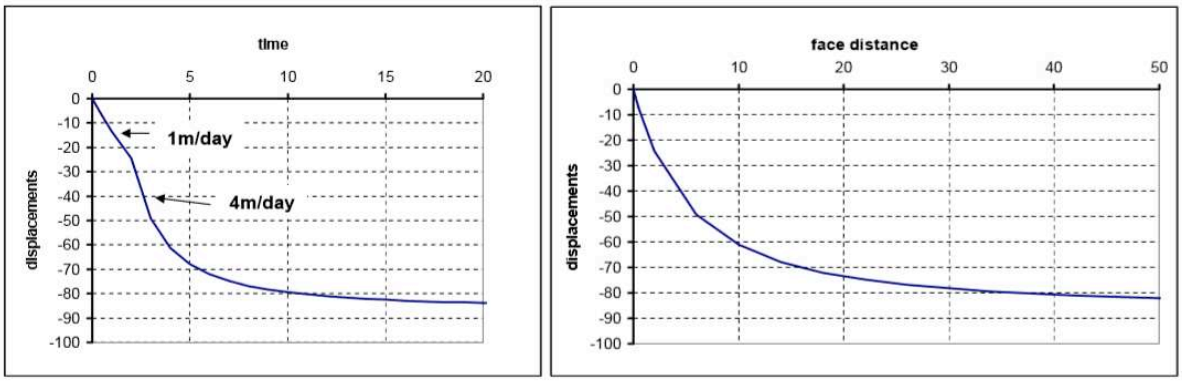

Figure 1 - Time-displacement diagram and distance-displacement diagram with excavation velocity change (Schubert, 2015).

2.1.2 Deflection lines and trend lines

Deflection lines are constructed by connecting displacements measures of all excavation extension in a certain time (OGG, 2014). The plot of these lines for several time intervals makes easy the spatial visualization of each component of displacement occurrence and the influence of advance on each instrumentation sections behind the face (Schubert & Grossauer, 2004). Onion-shaped curves are considered “normal” and deviations of this geometry or increase of the area between successive curves indicate different ground characteristics ahead (Figure 2).

Trend lines are constructed by connecting the values of the deflection curves which are at a constant distance from the face (OGG, 2014). Horizontal trend lines indicate "normal" behavior, and any deviation may indicate different conditions in the mass ahead (Figure 2).

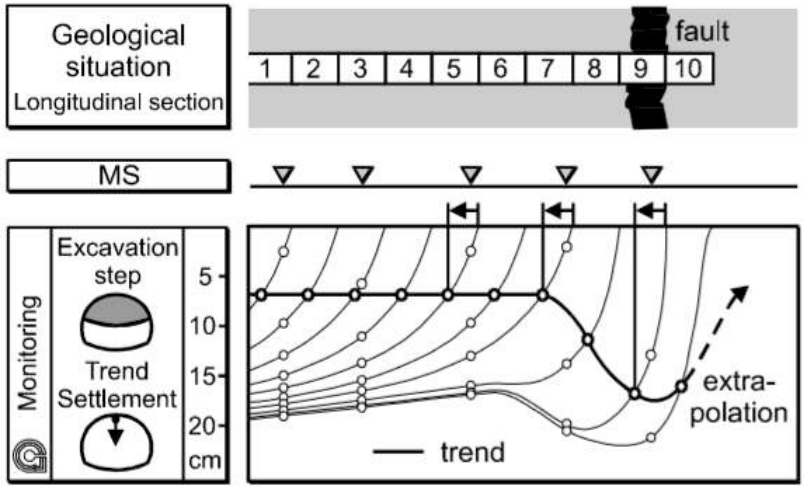

Figure 2 – Deflection lines and trend line approaching a fault zone (Steindorfer, 1998).

2.1.3 Displacement vector orientation

Displacement vectors can be presented in the cross section of the tunnel, plotting the radial displacements, or in the longitudinal, with the plot of vertical and longitudinal displacements (OGG, 2014), as can be seen in Figure 3. They allow evaluating the influence of the mass structure, system response and anisotropic displacements in the presented section (Schubert, 2015).

Not only the variation of the vectors in the section are evaluated, but also the orientation of these vectors, since deviations in the "normal" orientation are related to changes in the characteristics of the mass ahead of the excavation.

Jeon et al. (2005) consider the "normal" orientation of the displacement vector to be 15 ° with the vertical in the direction of the face of the tunnel, studies by Schubert et al. (2005) and Grossauer et al. (2008) show that, for the materials studied, the normal orientation of the displacement vector is about 10 °. However, what indicates variation of the mass behavior is not the absolute orientation of the displacement vector itself, but its variation, which is related to the stiffness contrast between materials and extension of the regions (Figure 4).

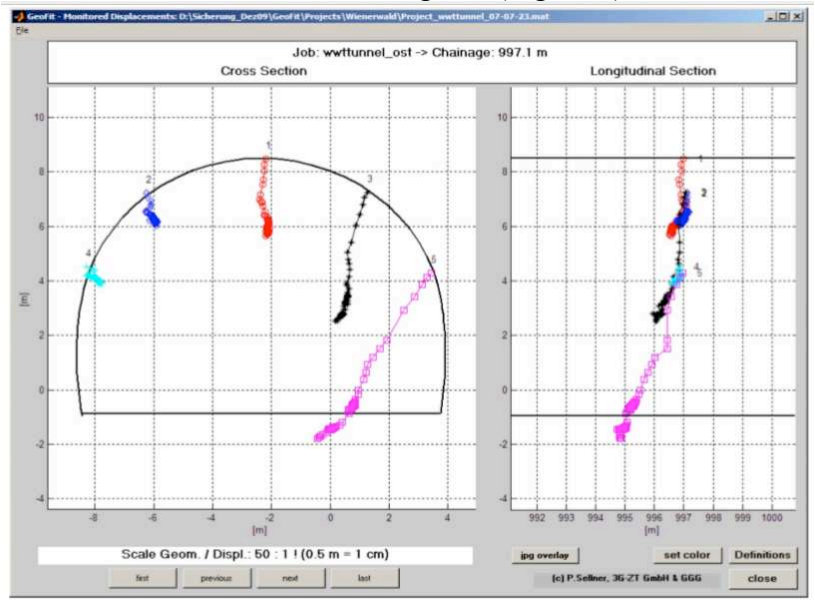

Figure 3 – Displacement vectors in cross section and longitudinal section (Schubert, 2015).

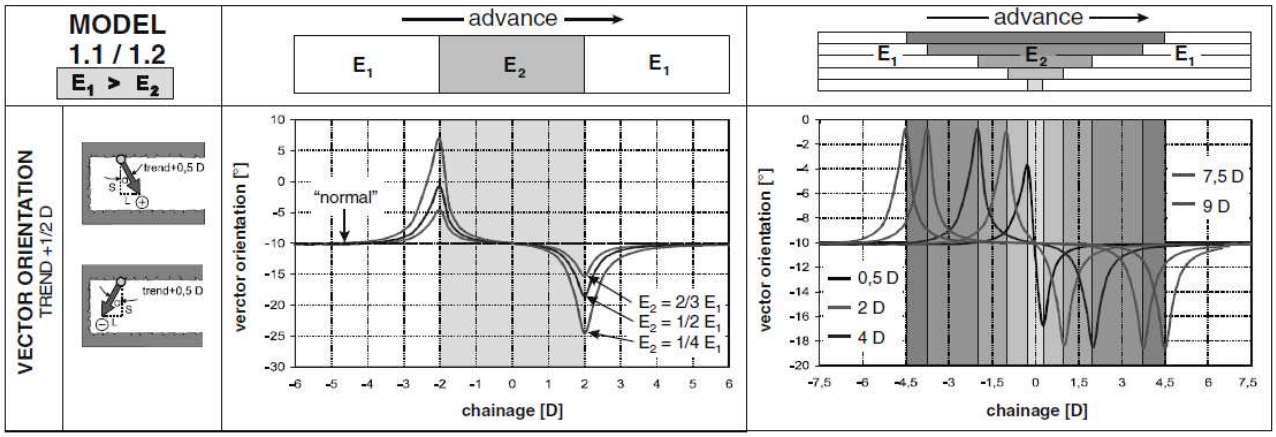

Figure 4 – Deviation of the displacement vector orientation from “normal” in response to crossing a weakness zone of different stiffness contrasts and zone lengths (Grossauer, 2001).

As can be seen in Figure 4, as the region of lower stiffness approaches, the orientation angle of the displacement vector (L / S) is increased by the greater longitudinal displacement that occurs due to the stress concentrations in the most competent mass. The opposite tendency, of decreasing angle, occurs when the excavation approaches a region with greater stiffness. Another way to see this is that the displacement vector orients in the direction of the excavation when the mass ahead is more competent, and against the excavation when the mass ahead is less competent.

2.1.4 Face extrusion

The face extrusion occurs by the three-dimensional effect of the redistribution of stresses in the mass with the excavation of the tunnel. The measurements are generally represented by graphs as a function of time or of the advance of the excavation for total cumulative extrusion and total differential extrusion (ITA, 2011). Extrusion data should be analyzed immediately after a reading because the face is more sensitive to destabilization than tunnel walls, enabling decision making and corrective measures to time (Lunardi, 2008). However, this is a parameter of difficult monitoring in the practice.

2.2 Negro et al. (2009) performance indicators

Negro et al. (2009) summarized a series of performance indicators for shallow tunnels. Some of them are presented in Table 1.

Table 1 - Performance indicators for shallow tunnels in soil (Negro et al., 2009).

Item	Symbol	Definition/Concept	Limiting Values	
			Serviceability	Ultimate State
a	Sc/D	Limiting crown settlement to tunnel diameter ratio	0,03 to 0,04	0,03 to 0,15
b	Ss/Sc	Limiting surface to crown settlement ratio at tunnel axis (or settlement increments ratio)	-	1,0
c	LDI	Longitudinal distortion index	-	Negative value
d	Uc	Dimensionless crown displacement	1,0	1,8

Limiting crown settlement to tunnel diameter ratios (Sc / D) were proposed based on centrifuge test data and the assessment of collapse cases in real tunnels.

The surface to crown settlement ratio at tunnel axis (Ss / Sc) tends to the unit in collapsed shallow tunnels as the cover mass slides toward the tunnel. This ratio must be taken into account together with other indicators since there are materials in which the displacement generates contraction of the mass, generating values greater than unity. Negro et al. (2009) also stress that the ratio of increments (ΔSs / ΔSc) is more adequate to verify the collapse condition.

Negro & Kochen (1985) and Horiuchei et al. (1986) independently proposed the longitudinal distortion index (LDI), which is defined by the derivative of the vertical displacements occurred in the longitudinal section of the tunnel, as described in Equation 1.

$$LDI(z) = \partial u(z)/\partial z \quad (1)$$

This indicator can be interpreted as a measure of shear strength mobilized by the material, and may be related to the stability condition of the mass. The LDI distribution can be approximated by a Gaussian distribution and if some instability process is initiated, this shape of the curve is modified, as can be seen in Figure 5.

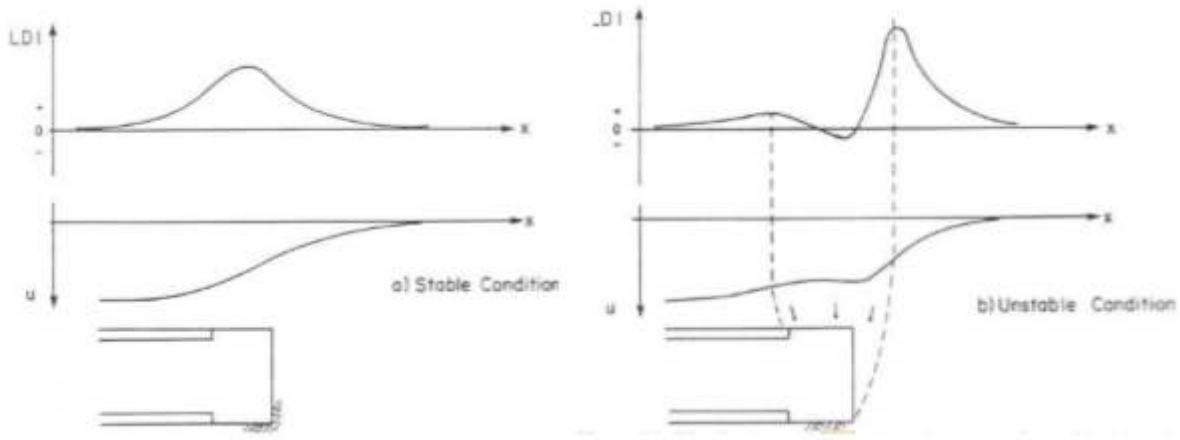

Figure 5 - LDI and settlement distributions for stable (a) and unstable (b) conditions (Negro et al., 2009).

The Dimensionless crown displacement is presented in Equation 2.

$$U_c = S_c E_{co} / D \sigma_{cro} \quad (2)$$

in which S_c is the crown settlement, E_{co} is the elasticity modulus of tunnel cover, D is the tunnel diameter and σ_{cro} is in situ radial effective stress in the tunnel crown.

The findings of Negro & Einstein (1991) are that dimensionless displacements of the ceiling of 1.8 generally imply a condition close to collapse, with development of concentration of shear stresses.

2.3 Sakurai (1981) critical strain

Sakurai (1981), because of the need to verify the stability of underground openings without a stress analysis, proposed the Critical Strain Assessment Technique. In this technique, the principal strain, ε_1, is compared with a limiting value, called critical strain, ε_0. This critical strain is calculated by the ratio between the uniaxial strength and the modulus of elasticity of the material, as observed in Equation 3.

$$\varepsilon_0 = \frac{\sigma_c}{E} \quad (3)$$

in which ε_0 is the critical strain, σ_c is uniaxial strength and E is modulus of elasticity.

Sakurai (1981), evaluating laboratory tests, observed that the critical deformation of rocks is usually between 0.1 and 1%. Latter, Chern et al. (1998), applying the concept of critical deformation in tunnels excavated in rocks in Taiwan, observed that deformations above 1% indicated stability problems, as can be observed in Figure 6.

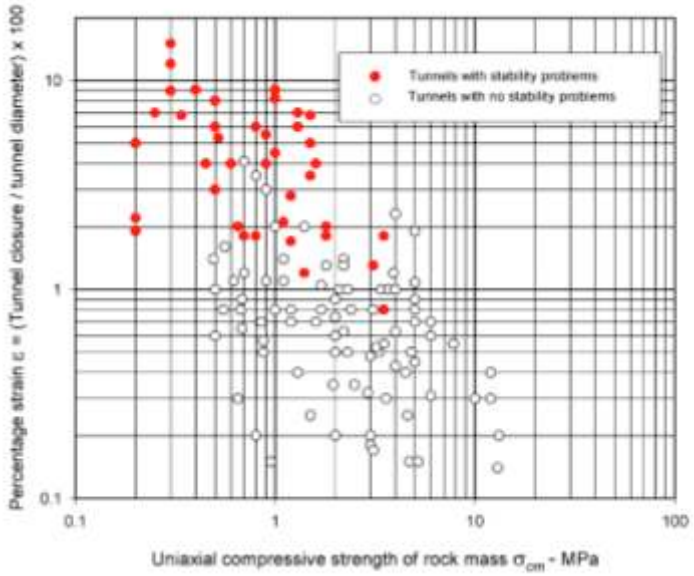

Figure 6 – Observed strains in tunnels Second Freeway, Pinglin e New Tienlun in Taiwan (Chern et al., 1998).

3 FINITE ELEMENT MODELING

The Finite Element software PLAXIS 3D Tunnel was adopted to calculate the displacements in each excavation step. It is a simple tool able to fulfill the objectives of the analysis, especially for the case where there are several phases for each simulation.

3.1 Model geometry and geology

The study covered 38 different types of geology, with four types of materials. Deep and shallow full face excavation tunnels of 10 meters of diameter were simulated, with overburden of 100 and 20 meters, respectively. The geologies are homogeneous and with zones of different materials of 1, 3 and 5 diameters of length, as can be observed in Figure 7.

The model section is 50 meters on the x-axis and 140 and 50 meters on the y-axis for deep and shallow tunnels, respectively. The model has 250 meters longitudinally, being the first 50 meters excavated in greater excavation steps, of 10 meters, and the following steps of 2.5 meters. Note that all output data were extracted in the internal 150 meters of the model, discarding the 50 meters closest to the boundaries.

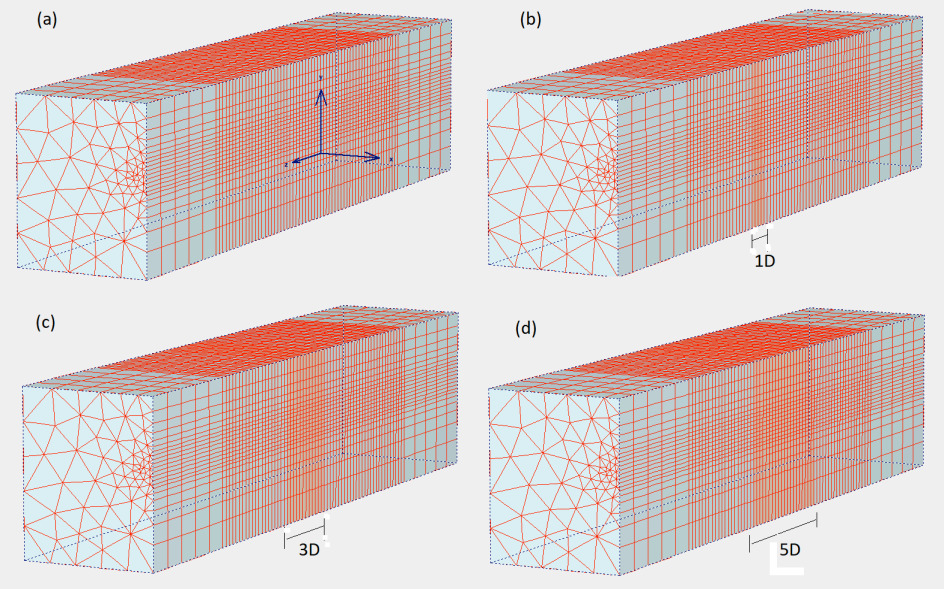

Figure 7 - Studied Geologies (a) homogenous (b) zone 2 of 1D length (c) zone 2 of 3D length (d) zone 2 of 5D length.

3.2 Materials

Several authors have adopted the linear-elastic constitutive model to simulate materials behavior with the objective of evaluating the behavior of transitions between materials, for example Tonon & Amadei (2000) and Yong et al. (2013), or even adopted the Mohr-Coulomb model only for the layer of different material within the mass, such as Jeon et al. (2005) and Grossauer (2001). However, these studies focused only on the prediction of the change of behavior of the mass, without studying the collapse, which is the objective of this work. Thereat, it was necessary to adopt a constitutive model with an adequate criterion of rupture for rocks, material to be simulated. The Hoek-Brown criterion was adopted, and it was necessary to convert these parameters to the Mohr-Coulomb criterion, model available in PLAXIS 3D Tunnel software.

The following parameters were estimated for the application of the Hoek-Brown criterion: specific weight (γ); modulus of elasticity of the rock mass (Em); poisson's ratio (ν); uniaxial compressive resistance of intact rock (σc); parameter of intact rock (mi); Geological Strength Index (GSI); Disturbance parameter (D). For the in situ stress state, the horizontal stress was assumed to be equal to the vertical stress.

The simulated materials are named as Good, Average, Bad and Poor Rock, nomenclatures related to the competence of each one. GSI reduction was applied to account fractures in the rock mass, and uniaxial strength reduction was applied to account on rock strength deterioration. Table 2 presents all parameters for each material.

Bad and Poor Rock parameters were selected to have poor support capacity, not being able to be excavated for great distances without support.

Table 2 – Materials parameters.

Material	K_0	γ (Kn/m^3)	mi	D	GSI	σ_{ci} (MPa)	E (GPa)	c (MPa)	$\Phi(^{o})$

Deep Tunnels									
Good	1	27	10	0	80	5.0	12.574	0.4549	39.0
Average	1	27	10	0	40	5.0	1.2574	0.2027	28.1
Bad	1	27	10	0	20	5.0	0.3976	0.1295	22.1
Poor	1	27	10	0	20	2.5	0.2812	0.0994	18.1
Shallow Tunnels									
Good	1	27	10	0	80	5.0	12.574	0.2802	49.6
Average	1	27	10	0	40	5.0	1.2574	0.0761	40.5
Bad	1	27	10	0	20	5.0	0.3976	0.0465	33.1
Poor	1	27	10	0	20	2.5	0.2812	0.0363	28.2

3.3 Cases and output

The 38 cases of study are presented in Table 3, in which collapse occurred in 8 cases.

Table 3 – Cases of study for deep and shallow tunnels.

Case	Material 1	Material 2	Zone 2 length	Chainage of collapse (m)	Case	Material 1	Material 2	Zone 2 length	Chainage of collapse (m)
Deep Tunnels					Shallow Tunnels				
TPGB	Good	-	-		TRGB	Good	-	-	
TPGBM1D	Good	Average	1D		TRGBM1D	Good	Average	1D	
TPGBM3D	Good	Average	3D		TRGBM3D	Good	Average	3D	
TPGBM5D	Good	Average	5D		TRGBM5D	Good	Average	5D	
TPGBR1D	Good	Bad	1D		TRGBR1D	Good	Bad	1D	
TPGBR3D	Good	Bad	3D		TRGBR3D	Good	Bad	3D	
TPGBR5D	Good	Bad	5D		TRGBR5D	Good	Bad	5D	
TPGBP1D	Good	Poor	1D		TRGBP1D	Good	Poor	1D	
TPGBP3D	Good	Poor	3D	120.0	TRGBP3D	Good	Poor	3D	115.0
TPGBP5D	Good	Poor	5D	110.0	TRGBP5D	Good	Poor	5D	115.0
TPGMB1D	Average	Good	1D		TRGMB1D	Average	Good	1D	
TPGMB3D	Average	Good	3D		TRGMB3D	Average	Good	3D	
TPGMB5D	Average	Good	5D		TRGMB5D	Average	Good	5D	
TPGMR1D	Average	Bad	1D		TRGMR1D	Average	Bad	1D	
TPGMR3D	Average	Bad	3D		TRGMR3D	Average	Bad	3D	
TPGMR5D	Average	Bad	5D		TRGMR5D	Average	Bad	5D	
TPGMP1D	Average	Poor	1D		TRGMP1D	Average	Poor	1D	
TPGMP3D	Average	Poor	3D	112.5	TRGMP3D	Average	Poor	3D	117.5
TPGMP5D	Average	Poor	5D	112.5	TRGMP5D	Average	Poor	5D	117.5

For all cases, displacements in the crown, invert, sidewall, points in the face (measurement of extrusion) and on the surface are the output evaluated. Time-displacement diagrams and distance-displacement diagrams were superseded by deflection curves, because the difference between are displacement increments, as in the diagrams.

For the points on the crown, floor and sidewall, the graphs of deflection curves with trend lines for the components in x, y and z of the displacements are generated. For points on the crown, graphs of trend lines are also plotted for the orientation of the displacement vector.

Finally, Negro et al (2009) performance indicators summarized in Table 1 and strains in the crown, floor and sidewalls are calculated and compared to the critical strain proposed by Sakurai (1981). Sakurai's critical strains were calculated assuming that there were no information about zone 2 parameters, what may happen in field, that's why critical strains were calculated for zone 1 material.

As a rule of thumb, increments of 20% where considered relevant.

4 RESULTS

4.1 Deflection lines and trend lines evaluation

As expected, deflection lines of crown, invert and sidewalls changed its shape after the excavation of the interface, as can be seen in Figures 8 to 15. However, these lines were not adequate to predict the change of material ahead of face, because substantial changes only occurred after the entrance on zone 2.

Five trend lines are presented, 5, 7.5, 10, 15 and 15 meters behind the face. Steeper changes of trend lines (TL) of vertical displacements of the crown may suggest near collapse states, as can be seen in Figures 8 to 11. Nevertheless, the association of collapse to displacements values is not an innovative practice, and, in the case of the simulations, higher displacements were expected in collapsing situations because of lower modulus of elasticity.

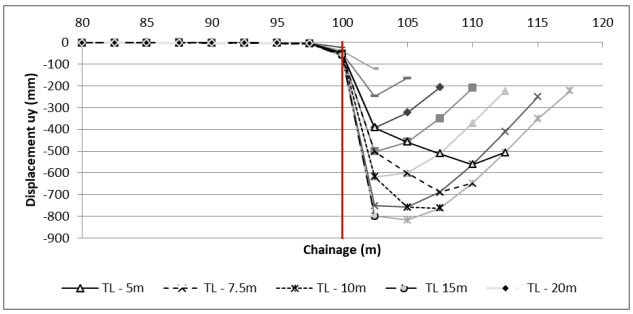

Figure 8 – TPBP3D crown vertical displacements deflection lines and trend lines.

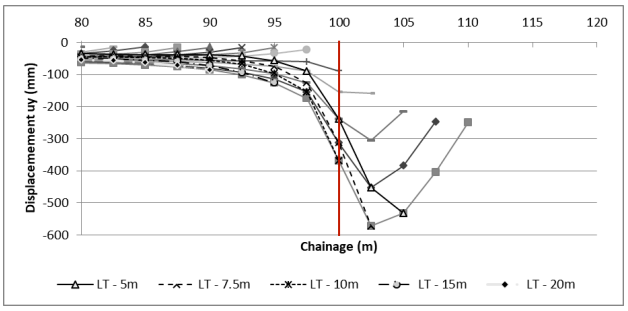

Figure 9 - TPMP3D crown vertical displacements deflection lines and trend lines.

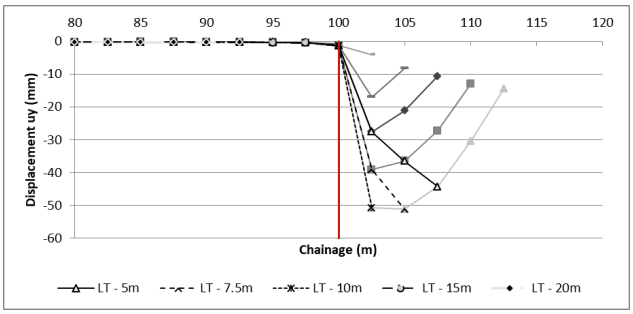

Figure 10 - TRBP3D crown vertical displacements deflection lines and trend lines.

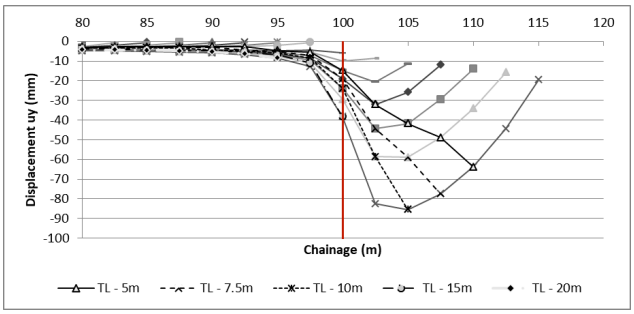

Figure 11 - TRMP3D crown vertical displacements deflection lines and trend lines.

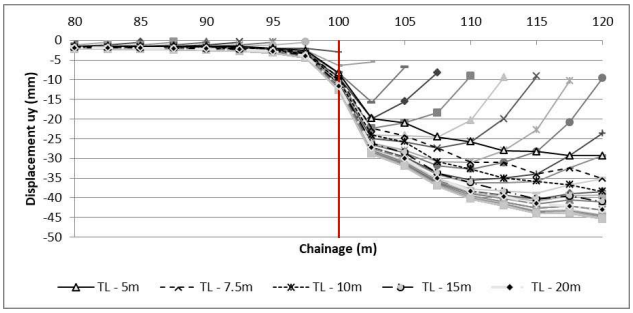

Figure 12 - TPBM5D crown vertical displacements deflection lines and trend lines.

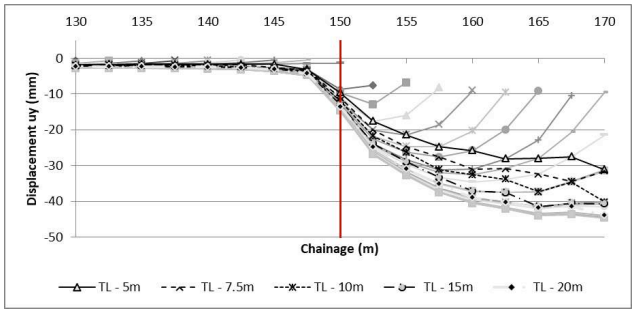

Figure 13 – TPMB5D crown vertical displacements deflection lines and trend lines.

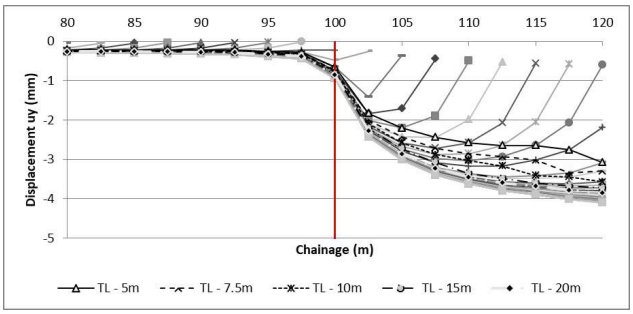

Figure 14 - TRBM5D crown vertical displacements deflection lines and trend lines.

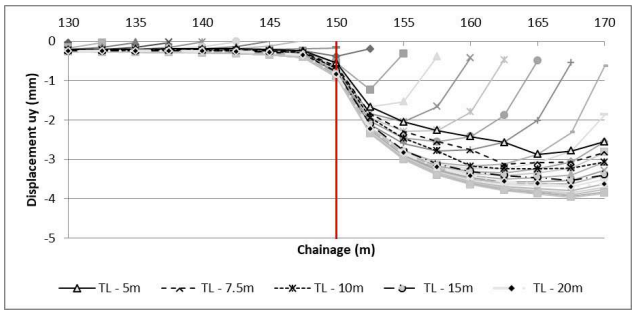

Figure 15 - TRMB5D crown vertical displacements deflection lines and trend lines.

Exemples of deflection lines and trend lines for other components and points are presented in Figures 16 to 19.

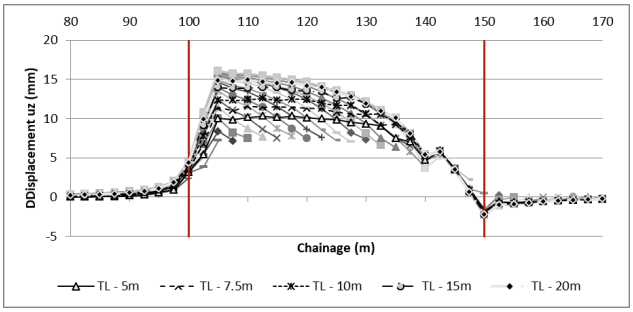

Figure 16 - TPBM5D crown longitudinal displacements deflection lines and trend lines.

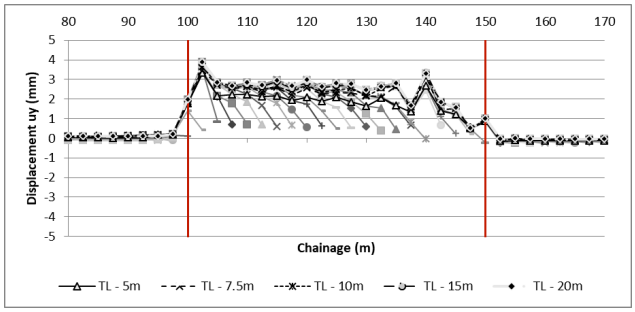

Figure 17 - TPBM5D sidewall vertical displacements deflection lines and trend lines.

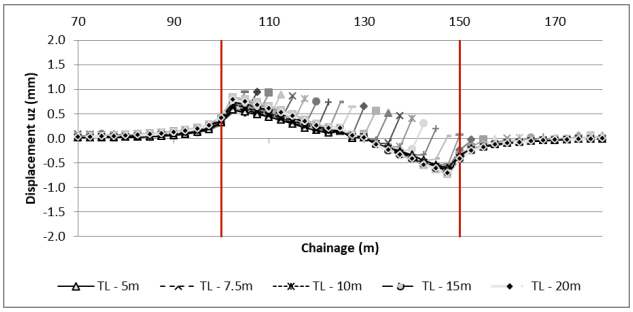

Figure 18 - TRBM5D crown longitudinal displacements deflection lines and trend lines.

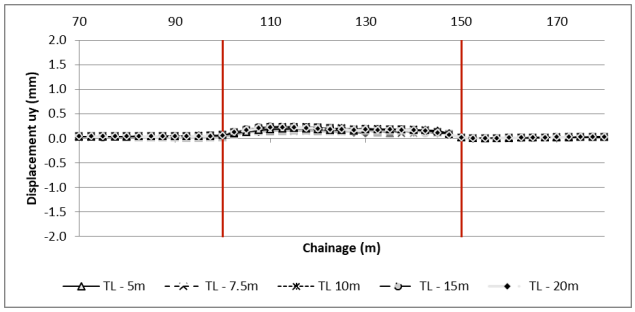

Figure 19 - TRBM5D sidewall vertical displacements deflection lines and trend lines.

4.2 Displacement vector orientation evaluation

"Normal" displacement vectors orientations were 0 º for Good Rock was 15 º for Average Rock, aligned with values found by other studies (Sellner & Steindorfer, 2000, Schubert et al. 2002, Jeon et al., 2005). In accordance with Jeon et al. (2005) and Orsini (2017), the displacement vector orientation was able to predict different mass behavior one to two diameters before the material transition, as can be seen in Figures 20 and 21.

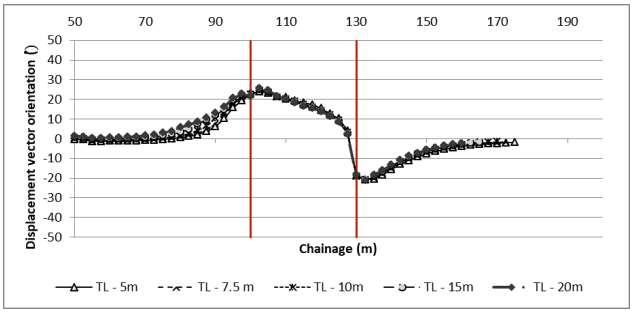

Figure 20 – TPBM3D crown displacement vector orientation trend lines.

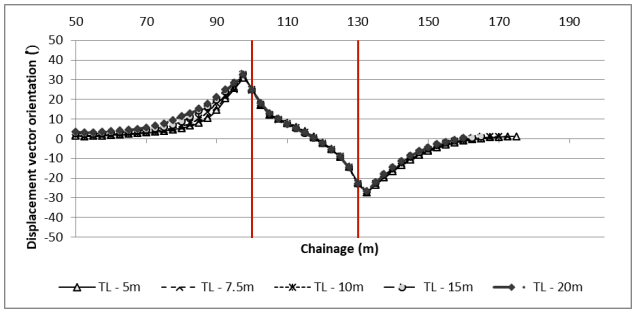

Figure 21 – TRBM3D crown displacement vector orientation trend lines.

Displacement vector orientations of collapsing tunnels present an increase still after the entrance of excavation in zone 2 (Figures 22 to 29). This behavior is a promising characteristic to be studied, but, care must be taken in the interpretation of this increase, because this can occur due approaching collapse or irregularity of lines (Figures 30 to 37). However, values lower than 20 º can be considered safe for tunnel construction, as seen be seen in Figures 22 to 37.

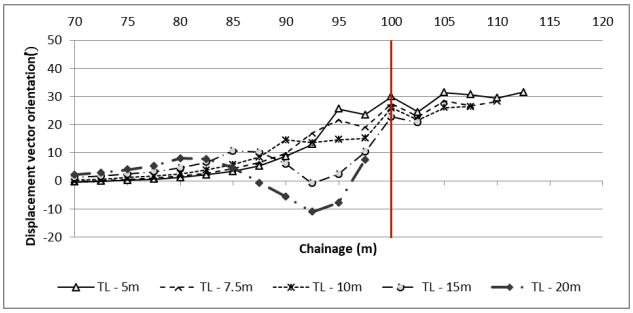

Figure 22 – TPBP3D crown displacement vector orientation trend lines.

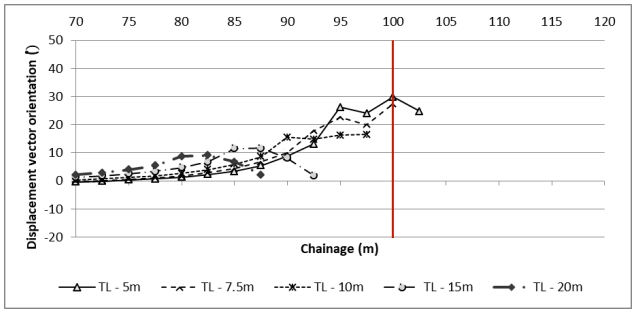

Figure 23 – TPBP5D crown displacement vector orientation trend lines.

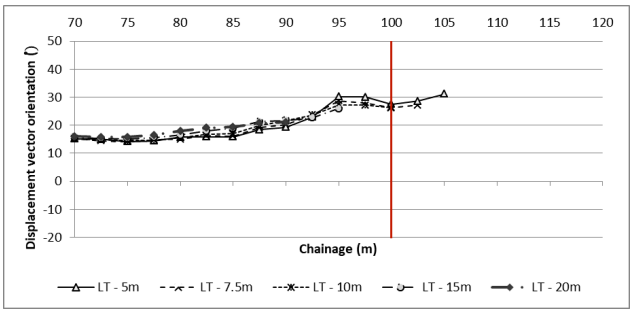

Figure 24 – TPMP3D crown displacement vector orientation trend lines.

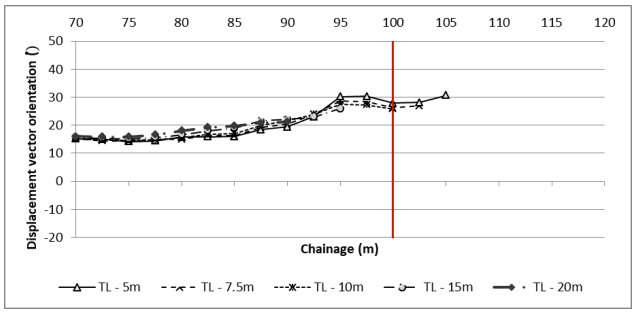

Figure 25 – TPMP5D crown displacement vector orientation trend lines.

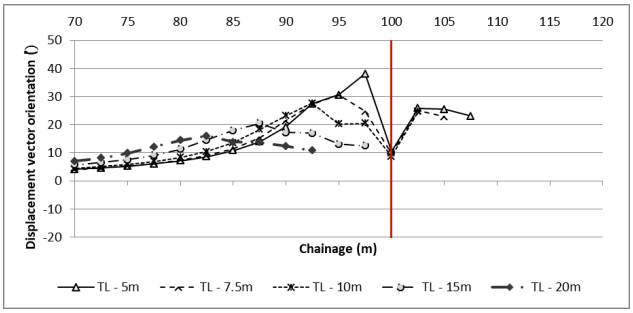

Figure 26 – TRBP3D crown displacement vector orientation trend lines.

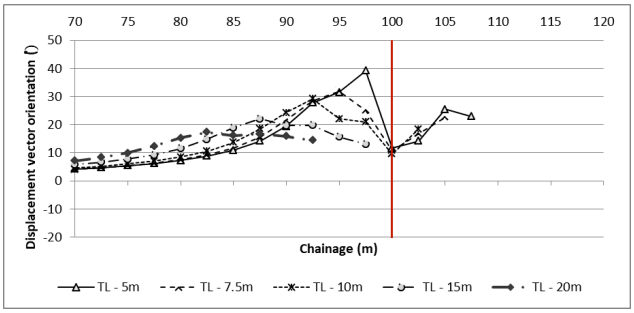

Figure 27 – TRBP5D crown displacement vector orientation trend lines.

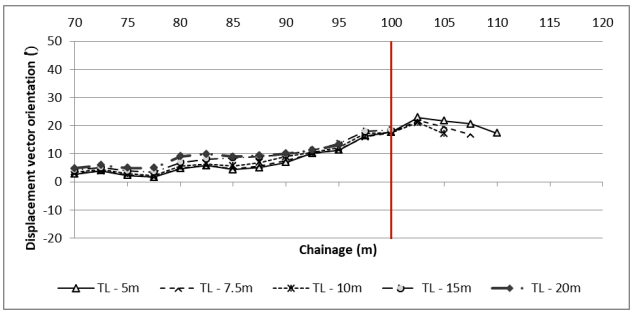

Figure 28 - TRMP3D crown displacement vector orientation trend lines.

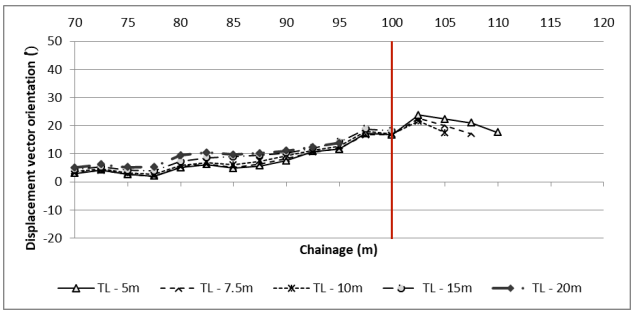

Figure 29 – TRMP5D crown displacement vector orientation trend lines.

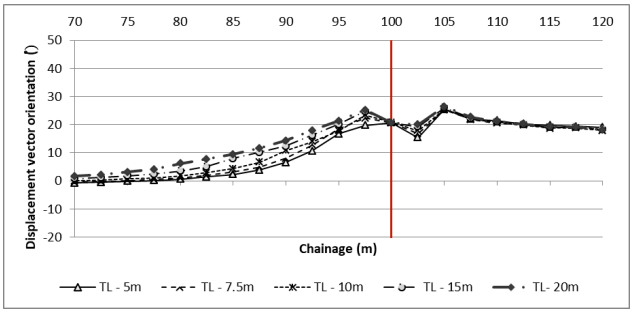

Figure 30 – TPBM5D crown displacement vector orientation trend lines.

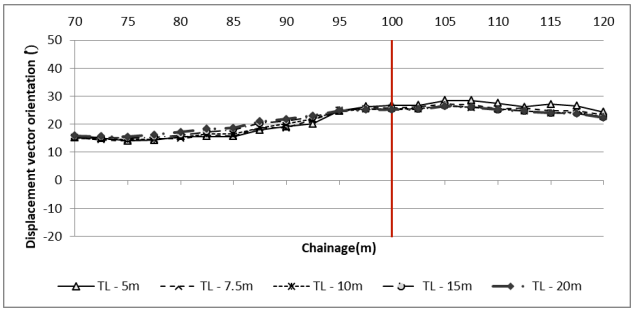

Figure 31 – TPMR5D crown displacement vector orientation trend lines.

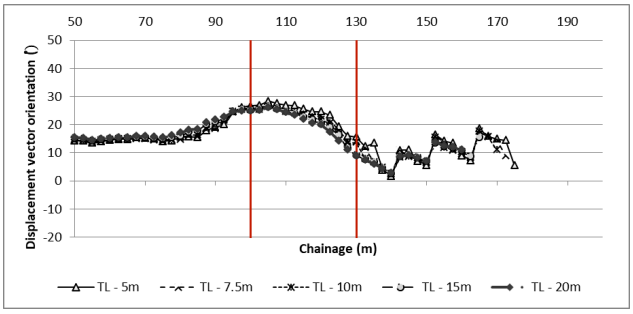

Figure 32 – TPMR3D crown displacement vector orientation trend lines.

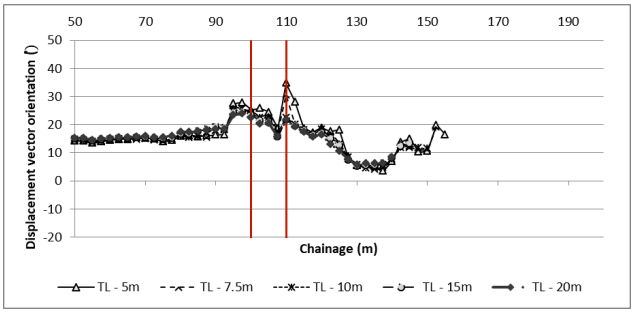

Figure 33 – TPMP1D crown displacement vector orientation trend lines.

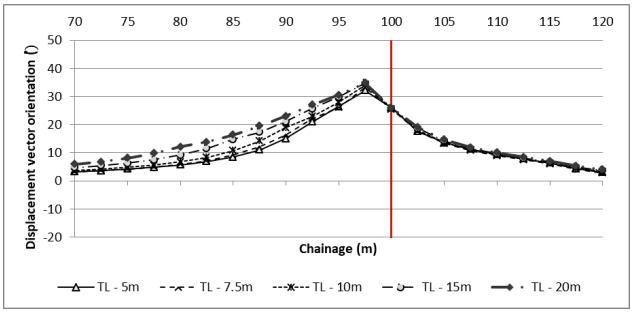

Figure 34 – TRBM5D crown displacement vector orientation trend lines.

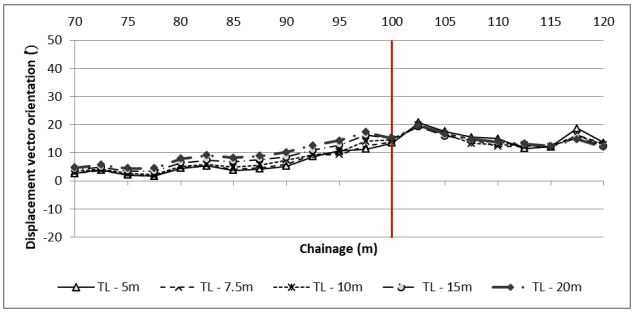

Figure 35 - TRMR5D crown displacement vector orientation trend lines.

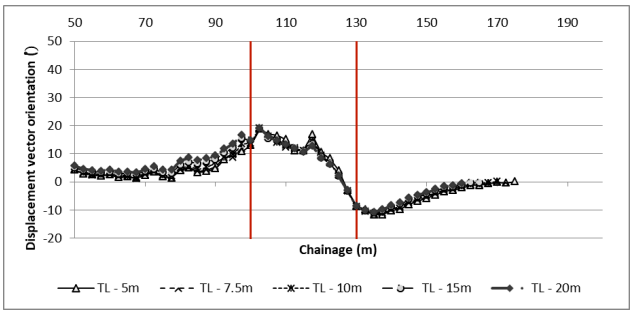

Figure 36 – TRMR3D crown displacement vector orientation trend lines.

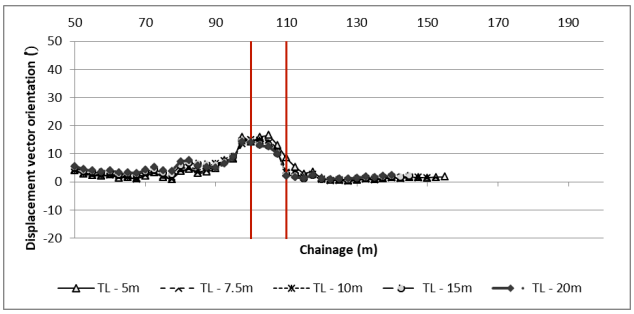

Figure 37 – TRMP1D crown displacement vector orientation trend lines.

4.3 Extrusion evaluation

High extrusion measurements were observed in all cases when entering a less competent material, as can be seen in Figures 38 to 41. However, in cases where collapse occurred, the increase of extrusion rate continued for several excavation steps after the entrance in zone 2 (Figures 38 and 40).

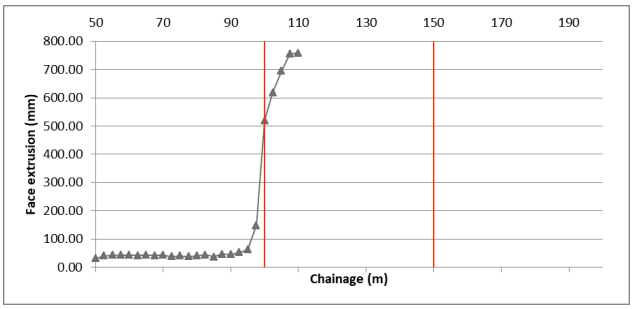

Figure 38 - TPBP5D face extrusion.

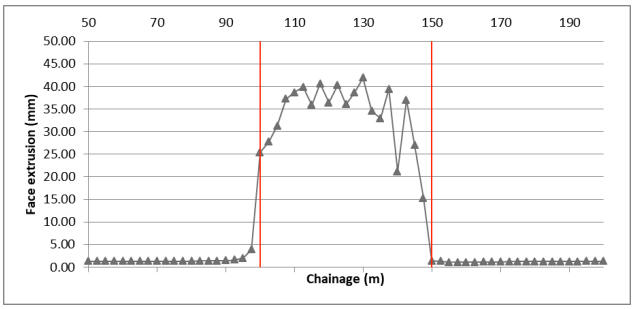

Figure 39 – TPBM5D face extrusion.

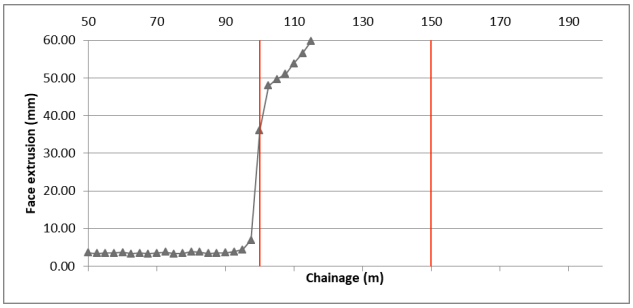

Figure 40 – TRMP5D face extrusion.

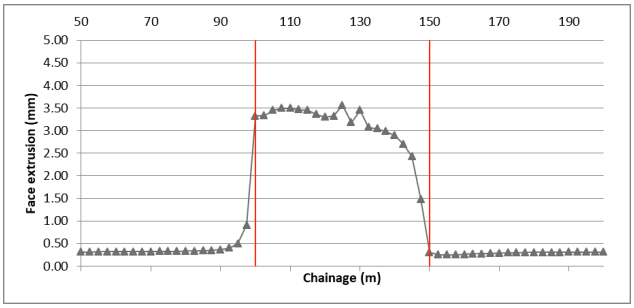

Figure 41 – TRBM5D face extrusion.

4.4 Negro et al. (2009) performance indicators evaluation

The crown settlement to tunnel diameter ratio reached the limiting value of 0.03 in 8 cases. All deep tunnels cases in which collapse occurred the limiting value was reached, but none of shallow tunnels cases reached the limiting value. Table 4 summarizes cases where the limiting value was reached and what chainage it occurred.

Table 4 – Cases in which the crown settlement to tunnel diameter ratio reached the limiting value.

Case	Chainage of collapse (m)	Uyt/D>0.03 starting at (m)
TPGBR5D		127.5
TPGBP3D	120.0	107.5
TPGBP5D	110.0	107.5
TPGMR3D		122.5
TPGMR5D		122.5
TPGMP1D		110.0
TPGMP3D	112.5	107.5
TPGMP5D	112.5	107.5

The surface to crown settlement ratio was only reached the value of 1 in the interface of materials for cases TRGBM1D and TRGBR1D.

The LDI at the surface was negative in many cases, but only homogeneous cases did not reach negative LDI at the crown. Figure 42 and Figure 43 presents examples of surface and crown LDI distributions. Negative LDI occurred right after the entrance in different material or far from the face, but collapse usually occurs near face, so a correction was made to consider only negative LDI one diameter behind the face.

Table 5 summarizes the behavior for deep and shallow tunnels simulated. The consideration of negative LDI occurring within one diameter behind the face successfully predicted the collapse of shallow tunnels. Only three cases of non-collapsing tunnels presented negative LDI values, but after the excavation of one to two diameters inside zone 2, LDI values became positive again.

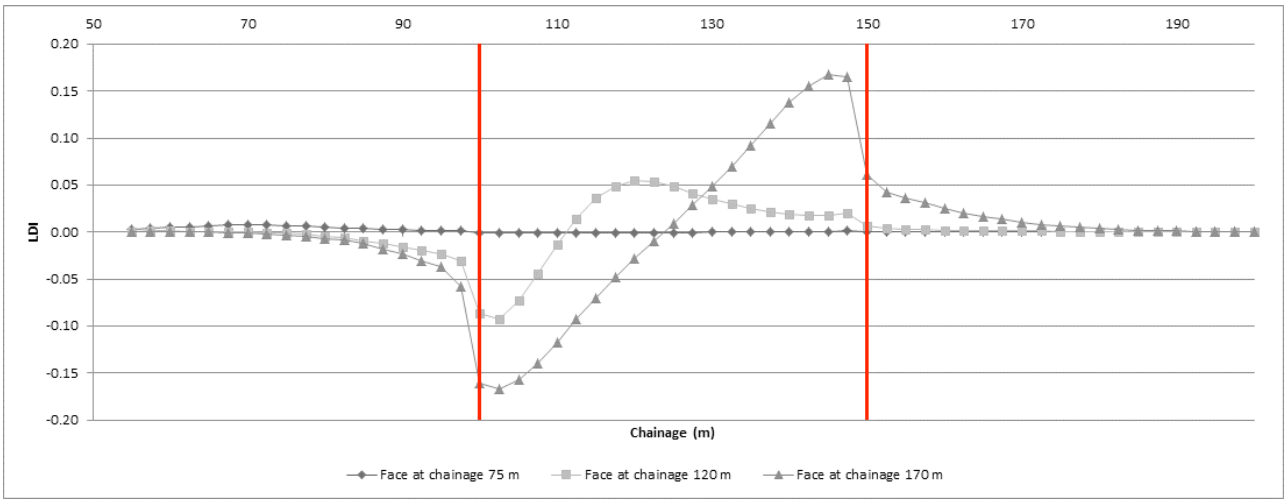

Figure 42 – Surface LDI distribution for case TRBM5D.

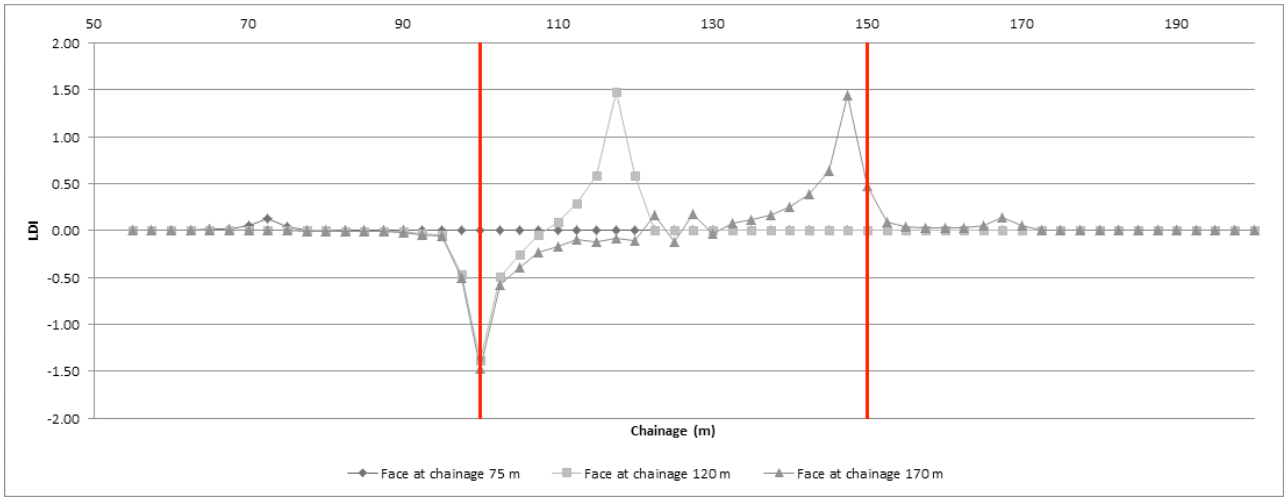

Figure 43 – Crown LDI distribution for case TRBM5D.

Table 5 – Surface and crown negative LDI occurrence.

Case	Chainage of collapse (m)	Surface LDI	Surface LDI 1D behind the face	Crown LDI	Crown LDI 1D behind the face
		Deep Tunnels			
TPGB					
TPGBM1D				x	until 105.0
TPGBM3D				x	until 110.0
TPGBM5D				x	until 115.0
TPGBR1D				x	until 105.0
TPGBR3D				x	until 112.5
TPGBR5D		x		x	until 110.0
TPGBP1D				x	until 112.5
TPGBP3D	120.0			x	until 110.0
TPGBP5D	110.0			x	until 110.0
TPGMB1D				x	x
TPGMB3D				x	x
TPGMB5D				x	x
TPGMR1D				x	x
TPGMR3D				x	until 110.0
TPGMR5D		x		x	until 110.0
TPGMP1D				x	until 110.0
TPGMP3D	112.5			x	until failure
TPGMP5D	112.5			x	until failure
		Shallow Tunnels			
TRGB					
TRGBM1D				x	until 112.5
TRGBM3D		x		x	until 115
TRGBM5D		x		x	until 115
TRGBR1D				x	until 110
TRGBR3D		x	until 120.0	x	until 115

Case	Chainage of collapse (m)	Surface LDI	Surface LDI 1D behind the face	Crown LDI	Crown LDI 1D behind the face
TRGBR5D		x	until 120.0	x	until 115
TRGBP1D		x	until 110.0	x	until 110
TRGBP3D	115.0	x	until failure	x	x
TRGBP5D	115.0	x	until failure	x	x
TRGMB1D		x		x	x
TRGMB3D		x		x	x
TRGMB5D		x		x	x
TRGMR1D		x		x	until 110
TRGMR3D		x		x	until 112.5
TRGMR5D		x		x	until 112.5
TRGMP1D		x		x	until 110
TRGMP3D	117.5	x	until failure	x	until failure
TRGMP5D	117.5	x	until failure	x	until failure

Obs: x = occurrence of negative LDI; until 110=occurrence of negative LDI until chainage 110 m.

Only homogeneous cases did not reach the limiting dimensionless crown displacement of 1.8. For deep tunnels, this value was too small, and reached in first excavations steps, but in shallow tunnels it was reached only after excavation entered zone 2.

4.5 Strains evaluation

All cases that collapse has occurred the strain was higher than 8% for deep tunnels, and higher than 1% for shallow tunnels. However, in cases with zones of poor rock of 1D length (TPGBP1D, TPGMP1D, TRGBP1D and TRGMP1D) high strains occurred, without the occurrence of collapse. In these cases, 3D stress distribution was sufficient to avoid collapse, but high strains still occurred.

Sakurai's (1981) critical strain where too conservative in all scenarios. The estimation of low uniaxial compressive strengths, 5 and 2.5 MPa, caused extremely small critical strains, situation that should not happen commonly on field, not aligning with values presented by Sakurai (1981) and Chern (1998). Critical strains calculated by Sakurai's technique and collapse strains are presented in Table 6.

Table 6 – Critical strains and maximum strains observed in each case.

Case	Chainage of collapse (m)	Sakurai (1981) critical strain	Maximum strain	Case	Chainage of collapse (m)	Sakurai (1981) critical strain	Maximum strain
Deep Tunnels				Shallow Tunnels			
TPGB		0.015%	0.039%	TRGB		0.012%	0.006%
TPGBM1D		0.015%	0.371%	TRGBM1D		0.012%	0.044%
TPGBM3D		0.015%	0.777%	TRGBM3D		0.012%	0.072%
TPGBM5D		0.015%	0.911%	TRGBM5D		0.012%	0.084%
TPGBR1D		0.015%	2.053%	TRGBR1D		0.012%	0.210%
TPGBR3D		0.015%	6.055%	TRGBR3D		0.012%	0.642%
TPGBR5D		0.015%	8.448%	TRGBR5D		0.012%	0.932%

TPGBP1D		0.015%	5.866%	TRGBP1D		0.012%	0.596%
TPGBP3D	120.0	0.015%	16.362%	TRGBP3D	115.0	0.012%	1.025%
TPGBP5D	110.0	0.015%	8.104%	TRGBP5D	115.0	0.012%	1.112%
TPGMB1D		0.054%	1.093%	TRGMB1D		0.026%	0.089%
TPGMB3D		0.054%	1.078%	TRGMB3D		0.026%	0.089%
TPGMB5D		0.054%	1.076%	TRGMB5D		0.026%	0.089%
TPGMR1D		0.054%	2.596%	TRGMR1D		0.026%	0.365%
TPGMR3D		0.054%	7.920%	TRGMR3D		0.026%	0.716%
TPGMR5D		0.054%	10.051%	TRGMR5D		0.026%	0.893%
TPGMP1D		0.054%	8.721%	TRGMP1D		0.026%	0.977%
TPGMP3D	112.5	0.054%	11.432%	TRGMP3D	117.5	0.026%	1.709%
TPGMP5D	112.5	0.054%	12.329%	TRGMP5D	117.5	0.026%	1.760%

4 CONCLUSIONS

Displacement monitoring plays an important role in on field tunnel stability verification. The main findings of the FEM simulations displacements evaluations were:

- Deflection lines and trend lines are interesting for overview of tunnel excavation, but do not predicts material transitions ahead. The inclination of trend lines can be studied to verify pre-collapse situations;
- Displacement vector orientations were the best indicator to predict the transition of materials, being able to predict the chance of behavior one to two diameters before the materials interface;
- Increases of displacement vector orientations were observed in collapsing cases, but it is difficult to predict failure from these increases because it may cause too many false alarms;
- The increase of extrusion rate maintenance for several excavation steps after the entrance in zone different material can be a sign of destabilization;
- For shallow tunnels, in which bigger surface settlements occurred, the LDI indicator successfully predicted the collapse.

REFERENCES

ITA. (2011). Monitoring and Control in Tunnel Construction. International Tunneling and Underground Space Association. ITA Working Group No. 2 Report n°009, Switzerland, 23 p.

Moritz, B., Koinig, J. & Vavrovsky, G.M. (2011). Geotechnical safety management in tunnelling – an efficient way to prevent failure. *Geomech. und Tunnelbau*, Vol. 4, p. 472–488.

Schubert, W. & Steindorfer, A. (2004). Selective displacement monitoring during tunnel excavation. *Felsbau*, Vol. 14, p. 93–97.

OGG. (2014). Geotechnical Monitoring in Conventional Tunneling Handbook. *Austrian Society for Geomechanics*, Austria, 90 p.

Schubert, W. & Grossauer, K. (2004). Evaluation and interpretation of displacements in tunnels. *14th International Conference on Engineering Surveying*, Zurich, p. 1–12.

Steindorfer, A. (1998). Short Term Prediction of Rock Mass Behaviour in Tunnelling by Advanced Analysis of Displacement Monitoring Data. Doctoral Thesis. Technical University Graz, Austria, p. 121.

Schubert, W. (2015). State of the art in tunnel monitoring. Austrian Tunnelling Seminar Ankara, Austria.

Jeon, J.S., Martin, C.D., Chan, D.H. & Kim, J.S. (2005). Predicting ground conditions ahead of the tunnel face by vector orientation analysis. *Tunn. Undergr. Sp. Technol*., Vol. 20, p. 344–355.

Schubert, W., Grossauer, K. & Sellner, P. (2005). Advances in the observational approach in tunnelling by new techniques of monitoring data evaluation. *10th ACUUS International Conference*, . Moscow State University of Civil Engineering, Moscow.

Grossauer, K., Schubert, W. & Lenz, G. (2008). Automatic displacement monitoring data interpretation – the next step towards an expert system for tunneling. *42nd US Rock Mechanics Symposium and 2nd U.S.-Canada Rock Mechanics Symposium*, San Francisco, CA, USA.

Lunardi, P. (2008). Design and Construction of Tunnels: Analysis of Controlled Deformations in Rock and Soils (ADECO-RS). *Springer Science & Business Media*. Milano, Italy, 576 p.

Negro, A., Karlsrud, K., Srithar, S., Ervin, M. & Vorster, E. (2009). Prediction, monitoring and evaluation of performance of geotechnical structures. *17th International Conference on Soil Mechanics and Geotechnical Engineering:* The Academia and Practice of Geotechnical Engineering, Vol. 4, p. 2930–3005.

Sakurai, S. (1981). Direct strain evaluation technique in the construction of underground openings. *22nd U.S. Symposium on Rock Mechanics*, Cambridge, MA, p. 278–282.

Orsini, B. de O. (2017). Inovação em Analise de Risco e Tomada de Decisão em Escavações em Túneis. Marter Dissertation, Departamento de Engenharia Civil e Ambiental, Universidade de Brasília, Brasília, DF, Brazil 96 p. (in Portuguese).

Grossauer, K. (2001). Tunnelling in Heterogeneous Ground - Numerical Investigation of Stresses and Displacements. Diploma Thesis,. Graz University of Technology, Graz, Austria, 56 p.

Negro, A. & Kochen, R. 1985. Discussion on Session III, Underground Construction and Building Foundations, *Symp. on Special Foundations*, ABMS/FAAP (Sao Paulo), Vol. 2, p.115-120 (in Portuguese).

Horiuchi, Y., Kudo, T., Tashiro, M. and Kimura, K. 1986. A shallow tunnel enlarged in diluvial sand. *World Tunnel Congress (ITA): Large Underground Openings* (Firenze), Vol. 1, p.752-760.

Chern, J.C., Yu, C.W., and Shiao, F.Y. (1998). Tunnelling in squeezing ground and support estimation. *Reg. Symp. Sedimentary Rock Engineering*, Taipei, 192-202.

Tonon, F. & Amadei, B. (2000). Detection of rock mass weakness ahead of a tunnel - a numerical study. *Pacific Rocks* 2000, Vol. 1, p. 105–111.

Yong, S., Kaiser, P.K. & Loew, S. (2013). Rock mass response ahead of an advancing face in faulted shale. *Int. J. Rock Mech. Min. Sci*., Vol. 60, p. 301–311.